THE JOURNAL OF PHYSICAL CHEMISTRY B

Article

Cite This: J. Phys. Chem. B 2019, 123, 170−179

pubs.acs.org/JPCB

Preferential Equilibrium Partitioning of Positively Charged Tryptophan into Phosphatidylcholine Bilayer Membranes

Cari M. Anderson,[†] Alfredo Cardenas,[‡] Ron Elber,[†,‡] and Lauren J. Webb*[,†,§,∥]

[†]Department of Chemistry, [‡]Institute for Computational Engineering and Sciences, [§]Institute for Cellular and Molecular Biology, [∥]Texas Materials Institute, The University of Texas at Austin, 2506 Speedway STOP A5300, Austin, Texas 78712, United States

ABSTRACT: The interactions between small molecules and lipid bilayers play a critical role in the function of cellular membranes. Understanding how a small molecule interacts with the lipid bilayer differently based on its charge reveals primordial mechanisms of transport across membranes and assists in the design of drug molecules that can penetrate cells. We have previously reported that tryptophan permeated through a phosphatidylcholine lipid bilayer membrane at a faster rate when it was positively charged (Trp+) than when negatively charged (Trp−), which corresponded to a lower potential of mean force (PMF) barrier determined through simulations. In this report, we demonstrate that Trp+ partitions into the lipid bilayer membrane to a greater degree than Trp− by interacting with the ester linkage of a phosphatidylcholine lipid, where it is stabilized by the electron withdrawing glycerol functional group. These results are in agreement with tryptophan's known role as an anchor for transmembrane proteins, though the tendency for binding of a positively charged tryptophan is surprising. We discuss the implications of our results on the mechanisms of unassisted permeation and penetration of small molecules within and across lipid bilayer membranes based on molecular charge, shape, and molecular interactions within the bilayer structure.

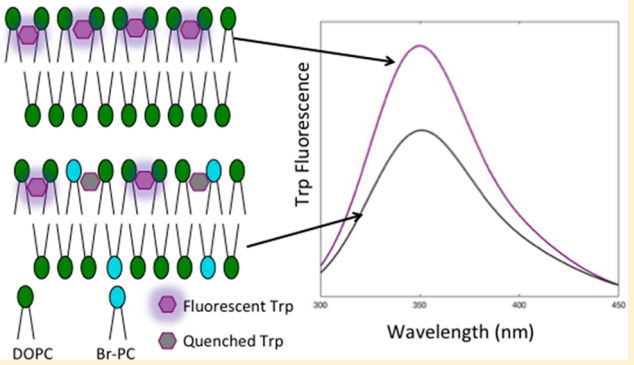

INTRODUCTION

One of the most important functions of the biological lipid bilayer membrane is to act as a barrier that selectively admits and excludes certain molecules based on the needs of the cell. Understanding how this occurs in the absence of protein machinery that has evolved to transport particular atoms or molecules across the bilayer is particularly important for several reasons. First, it is hypothesized that primordial cells existed for a significant period of time before the selective macromolecular machinery that aids in these processes evolved. Understanding the mechanisms of how primitive membranes could selectively transport beneficial molecules, such as nutrients, into the cell or waste out of the cell, while at the same time excluding toxic molecules, is essential for understanding this period of cellular evolution.[1−4] Second, therapeutic molecules introduced to an organism must eventually find their way to their target, which often means crossing a cellular membrane without a dedicated protein channel.[5] While the pharmaceutical industry has developed a range of empirical tools for guiding the design of molecules that will be effective in this regard,[6−9] understanding molecular-level mechanisms for this process would be beneficial in providing more quantitative guidance for drug design. Finally, any detailed understanding of molecular-level mechanisms of membrane behavior must include the ability to quantitatively model the membrane a priori, and understanding a process as simple as the transport of a molecule across that membrane must be adequately modeled by any level of theory which seeks to be acceptable to membrane researchers. For this reason, detailed investigations into the transport of small molecules across a lipid bilayer membrane are necessary. Experimental permeability experiments and molecular dynamic (MD) simulations have been performed for a range of solute molecules through a variety of lipid bilayers to compare how charge,[10] size,[11] and hydrophobicity[12−14] of molecules affect the ability to permeate a lipid bilayer membrane.[15]

This subject is of increased recent interest because of cell penetrating peptides (CPPs),[16−20] short (15−30 amino acids) peptides that carry large positive charges and penetrate the lipid bilayer through mechanisms that are still under investigation.[17−19] We have previously studied how changing the charge on the amino acid tryptophan, controlled by changing the protonation state of the backbone N and C termini through solution pH, affected the rate at which the charged amino acid permeated a zwitterionic phosphatidylcholine lipid bilayer.[21] Results from our previously published work demonstrated that positively charged tryptophan (Trp+, in which the carboxyl terminal of the tryptophan is protonated) permeated 120 nm diameter vesicles composed of 1,2-dioleoyl-

Received: October 9, 2018
Revised: November 19, 2018
Published: November 27, 2018

DOI: 10.1021/acs.jpcb.8b09872
J. Phys. Chem. B 2019, 123, 170−179

sn-glycero-3-phosphocholine (DOPC) at a faster rate than the negatively charged tryptophan (Trp−, in which the N terminal of the tryptophan in unprotonated) by a factor of approximately 10^8. Complementary MD simulations revealed that Trp+ also had a potential of mean force (PMF) barrier that was approximately 15 kcal mol^{-1} lower than that of Trp−. These experiments were conducted by spiking a solution of DOPC vesicles with a high concentration of the charged amino acid, then separating vesicles from solution through size exclusion chromatography over the time course of the experiment, and quantifying the amount of the charged tryptophan associated with the vesicle through fluorescence spectroscopy. We followed the association of the amino acid with the vesicle until no further changes in concentration were measured; this occurred after 4 h, but we confirmed there were no changes between 4 h and up to 1 week (at which point vesicles began to aggregate). In addition to faster interactions with the lipid vesicle, we also measured differences in the concentration of Trp+ and Trp− associated with the vesicle at equilibrium. These experiments were designed to test solely for permeation of the amino acid through the lipid bilayer and assumed that any tryptophan associated with the vesicle after the size exclusion column separation had been transported from outside to inside the vesicle.

Our experiments did not distinguish between tryptophan that permeated through the lipid bilayer from tryptophan that simply partitioned into the membrane and remained within the bilayer at equilibrium. However, in transmembrane proteins, tryptophan is commonly found at the membrane/water interface where it appears to serve a role of anchoring the protein within the bilayer, facilitated by the structure of the amino acid.[22−31] Tryptophan's hydrophobic indole ring orients in a position to be buried in the hydrophobic core of the lipid bilayer, whereas the polar amide backbone favors the lipid near-surface and headgroup region of the membrane. Because of this, tryptophan residues in transmembrane proteins are commonly found at the interfacial region, usually on the extracellular side of the membrane, but rarely at the center of the bilayer.[28,32,33] This is seen, for example, in gramicidin A (1GRM),[34] OmpF (20MF),[35] and the photosynthetic reaction center (1PRC).[36]

To determine whether charged tryptophan remains within the lipid bilayer at equilibrium or fully penetrates the membrane to the solvated vesicle interior, we have recently focused on measuring changes in the fluorescence energy of the tryptophan side chain as a function of time from an initial triggering event. The absorption and emission energy of tryptophan is sensitive to its environment,[37,38] a property that has been used extensively to determine the extent of hydration of tryptophan in a variety of biological contexts.[39,40] As shown in Figure 1, when dissolved in a hydrophobic solvent, such as hexanes, the maximum of the emission energy (λ_{max}) of tryptophan is ∼340 nm; this shifts to 380 nm when the amino acid is dissolved in water. The shift to lower emission energy in water versus a hydrophobic solvent is caused by the increased reaction field imposed on tryptophan in the high dielectric solvent, which stabilizes the excited state dipole moment of the molecule and lowers the transition energy.[38,39] When a solution of DOPC vesicles is spiked with tryptophan, the measurement of the fluorescence energy is a straightforward method to determine if tryptophan remains fully solvated (either outside or inside the vesicle) or is associated in some way with the more hydrophobic region of the interior of the bilayer, where the dielectric constant would be lower. As our system of vesicle-associated tryptophan is moved from one equilibrium condition to another, the fluorescence energy of the amino acid is a convenient tool for determining whether it is solvated in an aqueous or hydrophobic (i.e., lipid) environment.[37]

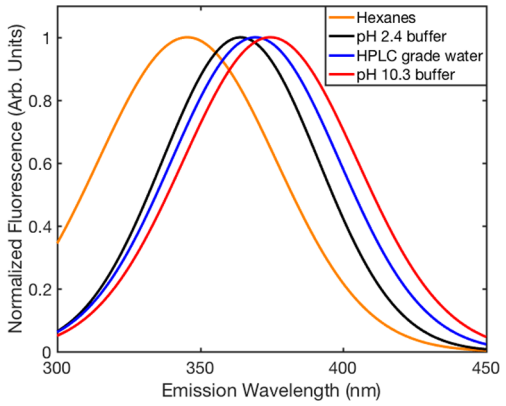

Figure 1. Tryptophan's emission spectra in different solvents. Hexanes (orange); pH 2.4 buffer (black); HPLC grade water (blue); and pH 10.3 buffer (red).

In order to determine where tryptophan resides within the membrane at equilibrium, it is also possible to add a fluorescence quencher to the structure of the bilayer itself by making vesicles containing 10−30 mol % of brominated DOPC lipids.[41−43] Bromine acts as a dynamic quencher for tryptophan that promotes intersystem crossing from the initial electronic excited state to a triplet state. Due to the slow emission from a triplet state, other collisional processes occur at a faster rate, resulting in quenching of the emission.[44] In previous studies, this property has been used to determine peptide and protein insertion depth within the membrane by changing the position of the Br along the fatty acid tail of the lipid and then measuring the extent of tryptophan quenching based on its proximity to the Br.[41,45−47]

In our previous work,[21] MD simulations and free energy calculations were performed on DOPC lipid bilayers, in which Trp+ and Trp− were moved from the fully solvated aqueous exterior to the middle of the membrane. The free energy calculations suggested that the glycerol backbone region is a favorable location for Trp+ to reside, similar to what is observed in pdb structures of tryptophan-containing transmembrane proteins. In contrast, Trp− experienced a slight decrease in free energy in moving from bulk water to the lipid phosphate group, but was positioned near the lipid headgroup where it remained largely solvated. These calculations suggested that the lowest free energy position for Trp+ versus Trp− differed by at least 4 Å, a significant distance in a fluorescence quenching experiment. For those reasons, we have made DOPC vesicles that incorporated 30 mol % brominated phosphocholine lipids (Br-PC) with bromine at positions 4 and 5 along the lipid tail, shown in Figure 2. The extent of quenching of tryptophan fluorescence was then a direct measurement of the extent of tryptophan partitioning into the lipid bilayer at equilibrium, and the role of the tryptophan charge in this process could be easily measured. We calculated the amount of quenching at each time point to track the migration of tryptophan from the glycerol backbone region to the bulk solution. When paired with the analysis of fluorescence emission spectra of tryptophan, this is a

DOI: 10.1021/acs.jpcb.8b09872
J. Phys. Chem. B 2019, 123, 170−179

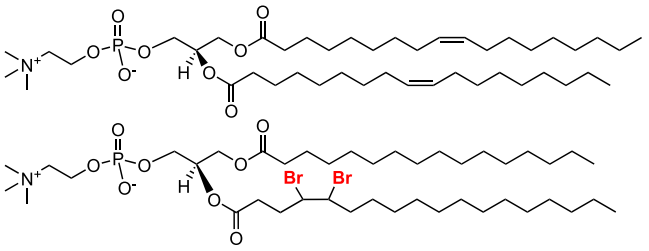

Figure 2. DOPC (top) and 1-palmitoyl-2-stearoyl(4,5)dibromo-*sn*-glycero-3-phosphocholine (Br-PC, bottom).

straightforward measurement for determining the extent of tryptophan partitioning in the lipid bilayer membrane.

The work described here for the first time differentiates between permeation across the lipid bilayer and partitioning into the bilayer structure itself for both positively and negatively charged tryptophan. Vesicles containing a fraction of Br-PC were incubated with excess Trp+ (pH 2.4) or Trp− (pH 10.3). After equilibration, vesicles were removed from the tryptophan-containing solution by size exclusion chromatography, and the fluorescence spectrum of tryptophan was monitored until the system returned to equilibrium, approximately 4 h. Changes in fluorescence energy and intensity were both related to the position of the amino acid in the bilayer/water system. We find that tryptophan does not permeate the membrane but actually partitions into the lipid bilayer structure, where it remains at equilibrium. Furthermore, we demonstrate that the concentration of Trp+ within the bilayer at equilibrium is 5 times higher than that of Trp−. Both experiment and simulations suggest that tryptophan resides near the glycerol linkage of the DOPC lipid, where it likely is stabilized by multiple electrostatic and hydrogen bonding interactions in the near-surface region of the membrane.

MATERIALS AND METHODS

Materials. DOPC (dissolved in chloroform) and 1-palmitoyl-2-stearoyl(4,5)dibromo-*sn*-glycero-3-phosphocholine (4,5-dibromo PC lipids, dissolved in chloroform) were purchased from Avanti Polar Lipids, Inc. and used without further purification. L-Tryptophan, sodium bicarbonate ($NaHCO_3$), and sodium carbonate anhydrous (Na_2CO_3) were purchased from Sigma-Aldrich. Sodium azide (NaN_3), citric acid monohydrate, and anhydrous sodium phosphate (Na_2HPO_4) were purchased from Fisher Scientific. All buffers were prepared using HPLC grade water purchased from Fisher Scientific. PD-10 desalting columns were purchased from GE Healthcare and used according to the manufacturer's instructions.

Vesicle Preparation. Because the charge of tryptophan was controlled by the pH of solution, two buffers were used for these experiments depending on the desired pH. For samples with Trp+, a buffer composed of 0.1 M citric acid and 0.1 M Na_2HPO_4 with 0.02% (w/v) NaN_3 at pH 2.4 was used. For samples with Trp−, a buffer composed of 0.1 M $NaHCO_3$ and 0.1 M Na_2CO_3 with 0.02% (w/v) NaN_3 at pH 10.3 was used.

Lipid films were prepared by drying appropriate aliquots of DOPC in chloroform under vacuum overnight. For quenching experiments, aliquots of DOPC in chloroform and Br-PC in chloroform were mixed to make a molar ratio of 70:30, respectively, before being placed under vacuum overnight. Lipid films that were not used immediately were stored in an air-free, N_2-purged glovebox for up to 1 week.

Vesicles were prepared using the extrusion method. In short, lipid films were hydrated with the appropriate amount of desired buffer to make 30 mM lipid solutions. Hydrated lipid films were vortexed for 5 min, freeze/thawed 12 times, and then passed through 100 nm pore polycarbonate membranes 12 times. The vesicle solutions were then stored in a 25 °C water bath until the fluorescence experiments were performed. The diameter of the prepared small unilamellar vesicles (SUVs) was confirmed using a Zetasizer Nano ZS for dynamic light scattering. Vesicles used for these experiments were 120 ± 20 nm in diameter. All vesicles were further characterized using atomic force microscopy to confirm spherical shape, Fourier-transform infrared (FTIR) spectroscopy to confirm no changes in gel-to-liquid phase transitions with the various buffers used,[48] and ^{31}P NMR spectroscopy with Pr^{3+} to confirm vesicles were all unilamellar (data not shown).[49] These characterization experiments clearly revealed that different buffers and pH did not alter the structure of the vesicles. Following literature precedent, we assume there is a homogeneous distribution of the Br-PC and DOPC lipids throughout the vesicles that contained the 70:30 (DOPC and Br-PC) lipid mixture.[41−43]

Vesicle Phase Transition Characterization. Infrared spectra of all of the vesicle samples were collected in a temperature controlled sample cell composed of two sapphire windows separated by 100 μm Teflon spacers in a Bruker Vertex 70 FTIR instrument. Spectra were averaged over 300 scans with 0.5 cm^{-1} resolution at temperatures ranging from 5 to 60 °C in 5 °C increments, and the background spectrum of the appropriate buffer for each temperature was subtracted. Each background subtracted spectrum was fit to a single Gaussian line shape with a custom least-squares fitting program to determine the peak center. The spectral peaks and shifts for the symmetric stretch of the polymethylene groups ($-CH_2$) at ~2850 cm^{-1} were analyzed to ensure there were no phase transitions at room temperature, and that all of the samples were in the liquid phase, rather than the gel phase.[48] If a phase transition is present, a shift of 0.5−3 cm^{-1} will be detected in the $-CH_2$ stretch spectra. No shifts in the FTIR spectra are indicative of no phase transitions.

Partitioning Experiments. A solution of 30 mM vesicles and a solution of 10 mM Trp+ or Trp− were mixed in a 1:4 ratio and allowed to equilibrate for at least 5 h. After equilibration, a PD-10 column equilibrated with the appropriate buffer was used to separate the vesicles from the reaction solution. Fluorescence spectra were collected on the vesicle solution every 10−20 min after elution for 4 h using a Fluorolog3 fluorimeter by exciting at 280 nm and collecting spectra from 300 to 450 nm in 1 nm increments. A 5 mm quartz cuvette (Starna Cells) was used for all samples.

To observe changes in tryptophan's environment over time, all of the fluorescence emission spectra, $F(x)$, were fit to a sum of two Gaussians, I_i, described in eq 1 as I_{lip} and I_{wat}

$$F(x) = I_{lip} + I_{wat} = a_{lip}[e^{-((x-b_{lip})/c_{lip})^2}] + a_{wat}[e^{-((x-b_{wat})/c_{wat})^2}] \quad (1)$$

where the subscripts lip and wat are representative of the environment of tryptophan in the lipid (I_{lip}) and water (I_{wat}) environment, respectively; a is a scaling factor; b_i is the λ_{max} of I_i; c is the variance of I_i; and x is the emission wavelength. These experiments were performed for samples at pH 2.4 and

DOI: 10.1021/acs.jpcb.8b09872
J. Phys. Chem. B 2019, 123, 170−179

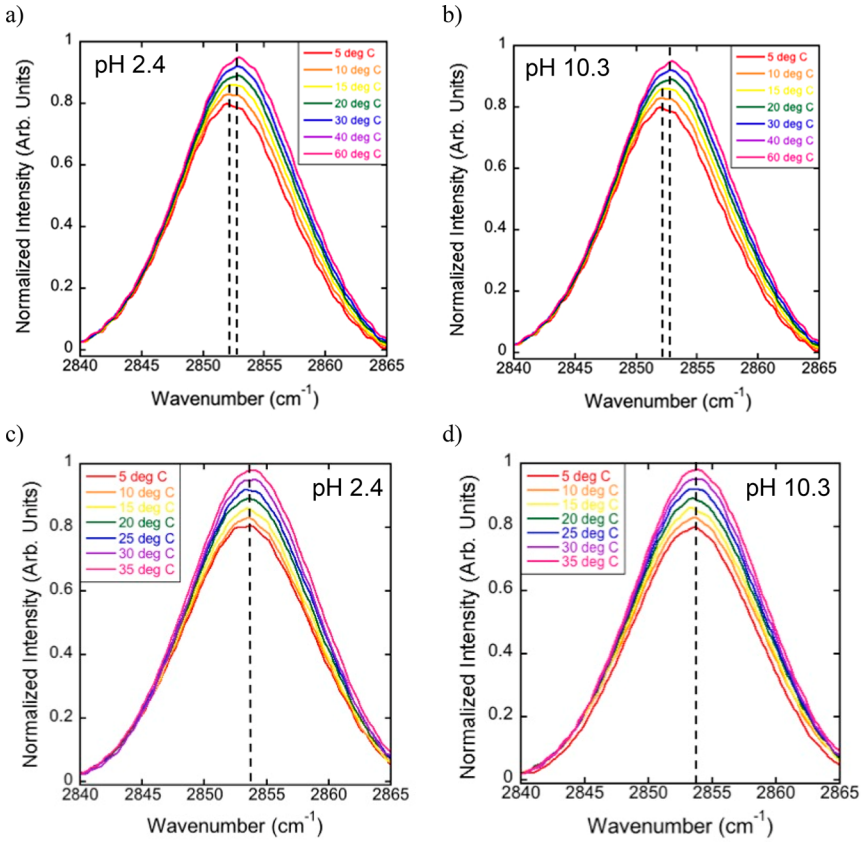

Figure 3. FTIR normalized spectra of the $-CH_2$ symmetric stretch at ~2853 cm^{-1} for vesicles used in the experiments. Spectra were collected at temperatures ranging from 5 (red) to 60 °C (pink) for 70:30 DOPC:Br-PC lipid vesicles and from 5 (red) to 35 °C (pink) for pure DOPC lipid vesicles. The dashed black lines illustrate the spectra maxima. (a) 70:30 DOPC:Br-PC lipid vesicles, pH 2.4; (b) 70:30 DOPC:Br-PC lipid vesicles, pH 10.3; (c) pure DOPC lipid vesicles, pH 2.4; (d) pure DOPC lipid vesicles, pH 10.3.

pH 10.3 for solutions with vesicles composed of 100 mol % DOPC and 70:30 mol % DOPC:Br-PC.

RESULTS

The goal of this work is to determine where a charged tryptophan molecule resides at equilibrium in a system composed of DOPC lipid vesicles and tryptophan, either solvated outside or inside the vesicle or alternatively, within the ~6 nm bilayer structure itself. This goal was informed by previous work that found that significant quantities of tryptophan associated with DOPC vesicles in a manner that depended on the charge of the tryptophan backbone. Our previous work only counted the presence of tryptophan associated in some way with the vesicle, and not whether it had permeated the vesicle by passing through the entire bilayer structure or partitioned into the bilayer structure at equilibrium. The goal of the present work is to determine the exact location of the tryptophan-vesicle system at equilibrium through measurements of tryptophan fluorescence energy and intensity.

To ensure that all of our vesicle solutions were consistent in size and shape, and that the phospholipids are in the liquid phase at room temperature, we used a rigorous characterization process briefly described in the Materials and Methods section. Because there has been no report on whether the gel-to-liquid phase transition temperature (T_m) of the system changed either as a function of the addition of the Br-PC lipid or by the change in pH, we used FTIR spectroscopy to ensure that the lipid tails were in the liquid disordered phase at room temperature for all of the samples we used in our experiments.[48] In Figure 3, we show FTIR spectra of the $-CH_2$ symmetric stretch at ~2853 cm^{-1} for temperatures ranging from 5 (red) to 60 °C (pink) for vesicles composed of 70:30 DOPC:Br-PC lipids at pH 2.4 and pH 10.3 in panels a and b, respectively. Because pure DOPC lipid vesicles have a known T_m of −20 °C at a neutral pH, we used a smaller temperature range of 5 (red) to 35 °C (pink) for the pure DOPC lipid vesicles at pH 2.4 and 10.3 in panels c and d, respectively. We observed a 0.5 cm^{-1} shift of the $-CH_2$ stretch from 2852.3 to 2852.8 cm^{-1} between 10 and 15 °C for the 70:30 DOPC:Br-PC lipid vesicles at both pH 2.4 and pH 10.3, indicative of a phase transition of the lipid tails. There were no further shifts detected from 15 to 60 °C, and no differences between pH 2.4 and 10.3 were detected. We conclude that at the temperatures at which our experiments were conducted, vesicles composed of both pure DOPC and 70:30 DOPC:Br-PC are in the liquid phase and well mixed.

In Figure 1, we show the normalized emission spectra of tryptophan dissolved in the two buffers used in this study, pH 2.4 (Trp+, black) and pH 10.3 (Trp−, red). There was a slight difference in fluorescence energy in these two buffers, with tryptophan emitting at 362 nm in the pH 2.4 buffer but at 370 nm in the pH 10.3 buffer. This is important for two reasons. (1) To quantify the extent of charged tryptophan partitioning into the lipid bilayer membrane, it was necessary to prepare a calibration curve for each buffer. More importantly, (2) if tryptophan moved from the lipid interior, characterized by an emission energy near 340 nm (similar to that when dissolved

DOI: 10.1021/acs.jpcb.8b09872
J. Phys. Chem. B 2019, 123, 170−179

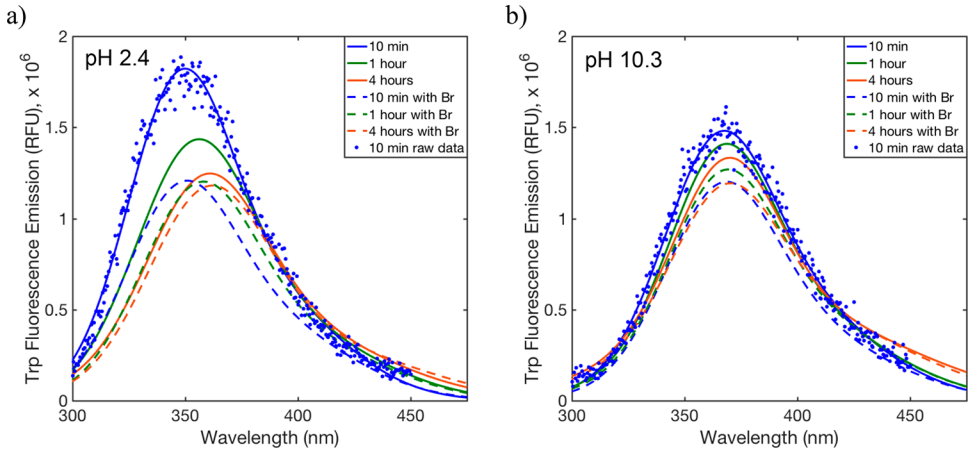

Figure 4. Representative spectra from selected time points for DOPC vesicles both with (dashed lines) and without (solid lines) Br-DOPC lipids. Spectra are shown at 10 min (blue), 1 h (green), and 4 h (red) after tryptophan-containing vesicles were re-equilibrated in a buffer without tryptophan. Filled circles show representative raw data from the 10 min time point as an example. (a) Spectra collected at pH 2.4 (Trp+), (b) spectra collected at pH 10.3 (Trp−).

in hexanes in Figure 1, orange), this would cause a large decrease in emission energy as tryptophan moved to the hydrophilic, aqueous environment. Therefore, changes in the absolute value of emission energy, as well as intensity, can be used to infer the local environment of each tryptophan at equilibrium and differences in the extent of equilibrium for Trp+ versus Trp−.

To determine a more exact location of tryptophan in the lipid bilayer at the time of elution from the column, we used fluorescence quenching with the Br-PC lipids shown in Figure 2, where the Br atoms are located close to the glycerol backbone region without disrupting the structure of the lipid. Representative emission spectra of tryptophan are shown in Figure 4, fitted to the sum of two Gaussians, as described by eq 1, at times of 10 min (blue), 1 h (green), and 4 h (red) after the sample was eluted from the size exclusion column for Trp+ (pH 2.4) and Trp− (pH 10.3). Representative raw data are also shown for the 10 min time point (blue dots) to demonstrate that our fitting procedure in eq 1 was able to accurately represent our raw data well. Solid lines depict spectra collected from pure DOPC lipid vesicles, while dashed lines are those of samples that contained 70:30 DOPC:Br-PC lipid vesicles. With our experimental design, 0 min was defined as the start of the column elution; at this time, the only tryptophan present in the sample was associated in some way with the vesicle in order to be collected by size exclusion chromatography. Although we measured fluorescence spectra up to 24 h after vesicles were removed from the spiked tryptophan solution, no further changes were observed after 4 h, and so we only show data up to 4 h here. It is important to note that the data shown in Figure 4 are for unnormalized spectra. The amount of tryptophan present in each sample was determined by comparing the 4 h time point data (when the majority of the tryptophan was in the bulk solution) to calibration curves created for Trp+ and Trp− in the respective buffer solutions. Due to the differences in the calibration curves for Trp+ and Trp−, the intensities of the pH 2.4 and pH 10.3 data cannot be directly compared to one another. At the time of column elution, there was 5 times more Trp+ than Trp− in the samples. We will comment on this further in the discussion. There are four observations to address in Figure 4: (1) the fluorescence emission spectra of tryptophan red-shift over time, but in ways that are significantly different for Trp+ versus Trp−; (2) the amount of fluorescence quenching of Trp+ at short time points is significantly greater compared to Trp−; (3) the total loss of fluorescence quenching over time is significantly different for Trp+ versus Trp−; and (4) there is an overall loss of fluorescence intensity over time, but to a greater degree for Trp+ compared to Trp−. These observations are discussed below.

Figure 4 shows that the emission spectra of both positively and negatively charged tryptophan shifted to lower energy over the 4 h of observation time; however, the shift was significantly larger for Trp+ than Trp−. At pH 2.4 with Trp+ (Figure 4a), there was a 12 nm shift in λ_{max} from 350 nm at 10 min to 362 nm at 4 h. In contrast, at pH 10.3 with Trp− (Figure 4b), the initial fluorescence energy measured 10 min after column separation was 368 nm, and shifted only to 370 nm over 4 h of observation. The significant blue shift shown by Trp+ 10 min after equilibration compared to Trp− demonstrates that significantly more Trp+ was exposed to a more hydrophobic environment at this initial time point, indicating that the equilibrium position for Trp+ in the tryptophan-spiked buffer was residing inside the membrane bilayer structure. Trp− was associated with the lipid bilayer at the time of column elution, but the lack of blue-shifting in the emission spectra tells us that it was further from the hydrophobic core and was closer to the water interface. At both pH values, after 4 h, the measured λ_{max} was equal to that of tryptophan in each respective buffer (shown in Figure 1), indicating that after 4 h of equilibration in buffer, essentially all tryptophan was solvated in bulk solution rather than associated with the lipid bilayer.

A second observation in Figure 4 is that the amount of tryptophan fluorescence quenching in the presence of 30 mol % Br-PC lipids (dashed lines) was significantly different for the positively and negatively charged molecule, with Trp+ showing significantly more quenching when exposed to the Br-PC lipids at short equilibration times. To compare the fluorescence emission spectra of Trp+ and Trp− in the absence and presence of the 30 mol % Br-PC lipids at each time point shown in Figure 4, we calculated the percentage of fluorescence quenching by determining λ_{max} for each of the fitted spectra in Figure 4, then divided the λ_{max} of $F(x)$ of the 70:30 DOPC:Br-PC vesicle samples by the λ_{max} of $F(x)$ of the

DOI: 10.1021/acs.jpcb.8b09872
J. Phys. Chem. B 2019, 123, 170−179

pure DOPC vesicle sample from the same pH and time point. As previously stated, there are different amounts of Trp+ and Trp− associated with the vesicles at the time of elution. The calculated percentages of quenching are relative to the amount of Trp+ or Trp− present in the sample at the time of elution. As shown in Figure 4 and Table 1, when the first time point was collected at 10 min, 34% of the Trp+ contained in the sample was quenched, compared to only 18% of Trp−. This indicates that more Trp+ was present within the structure of the lipid bilayer and near enough to the Br to be quenched, while any Trp− in the sample was located further away from the Br atoms and less significantly affected by the quenching Br atoms. Because only 30 mol % of the lipids were Br-PC (and therefore capable of quenching tryptophan fluorescence), these calculated percentages of quenched fluorescence of Trp+ and Trp− at each time point represent the lower bound of the actual amount of tryptophan partitioned near enough to the glycerol backbone to interact with the Br. The percentages reported are representative of the population of tryptophan molecules close to the Br atoms. Fluorescence that is not quenched or experiences a lesser degree of quenching is due to tryptophan being further from Br atoms; this is either because tryptophan is in the bulk solution or still buried in the bilayer but further away from the Br-PC lipids laterally or vertically. While the difference in the fluorescence energy of Trp+ and Trp− suggests that Trp+ is more strongly solvated in the low dielectric lipid environment, the greater quenching of Trp+ demonstrates that the positively charged molecule resides closer to the glycerol linkage than Trp−, and thus closer to the quenching Br atoms. However, at the time of elution, Trp− remained associated with the lipid bilayer and therefore capable of passing through the size exclusion column with the vesicle sample. The reduced blue-shifting of Trp− emission spectra and the lower percentage of quenching compared to Trp+ indicates that any Trp− associated with the lipid bilayer at the time of column elution was further away from the quenching Br atoms and, thus, closer to the lipid headgroup/water interface. We will address this further in the discussion when we compare these observations to previously published computational results.

Table 1. Percent Quenching of Tryptophan Fluorescence in the Presence of 30 mol % Br-PC

time	pH 2.4	pH 10.3
10 min	34%	18%
1 h	16%	10%
4 h	5%	10%

When evaluating the amount of fluorescence of Trp+ and Trp− over time in the presence of 30 mol % Br-PC (Table 1), we see almost 100% fluorescence recovery for Trp+ and Trp− over the 4 h of observation. This recovery of fluorescence can be attributed to tryptophan re-equilibrating with the surrounding bulk solution, and thus further away from the Br atoms within the bilayer. There is more Trp+ fluorescence recovery, again indicating that the Trp+ associated with the lipid bilayer at 10 min was closer to the Br residues than the Trp− at 10 min because the quenching capability of Br is distance dependent. Since there was no tryptophan in the surrounding bulk solution at time 0, the tryptophan that was partitioned in the lipid bilayer exits the membrane for the bulk solution to re-equilibrate.

There was an evident loss in the intensity of λ_{max} over time for both Trp+ and Trp− in pure DOPC vesicles. There was a 32% decrease in the intensity of λ_{max} for low pH (i.e., Trp+, Figure 4a, solid lines) and 10% decrease for high pH (i.e., Trp−, Figure 4b, solid lines) when comparing the intensities of λ_{max} from 10 min to 4 h. Moreover, by 4 h after elution from the column, almost all of the Trp+ and Trp− was resolvated in the bulk buffered solution. Control experiments of tryptophan fluorescence in solution demonstrated that this loss in fluorescence intensity was not due to photobleaching; rather, the fluorescence quantum yield of tryptophan in aqueous environments was lower than in hydrophobic environments. This observation is indicative of more Trp+ associated with a more hydrophobic environment when the sample was initially eluted from the size exclusion column. In the case of Trp−, there was a significantly smaller change in the fluorescence intensity from 10 min to 4 h after elution. This is indicative of Trp− being in a more hydrophilic environment as soon as it is eluted from the size exclusion column and, thus, associated with the vesicle near the lipid headgroup/water interface. The observed loss in fluorescence intensity further demonstrates the migration of tryptophan from the interfacial region of the lipid bilayer to the bulk aqueous solution.

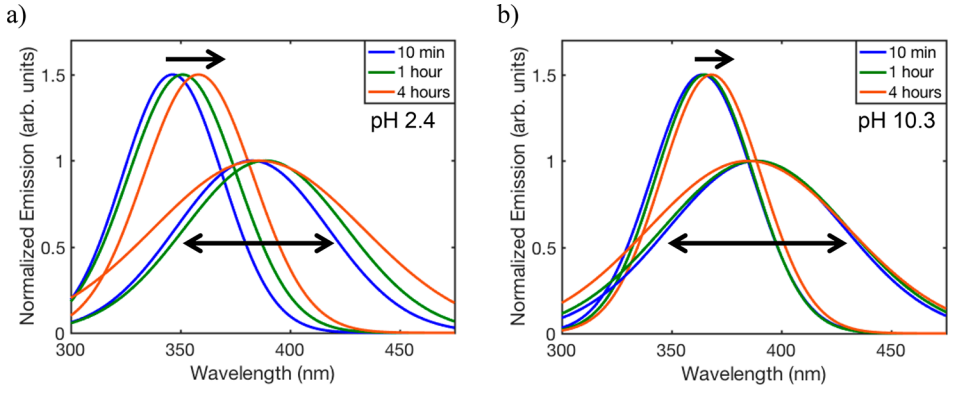

Figure 5. Normalized Gaussians I_{lip} (shorter wavelengths) and I_{wat} (longer wavelengths) from selected time points for DOPC vesicles with partitioned charged tryptophan. I_{lip} spectra are normalized to 1.5 maxima, and I_{wat} spectra are normalized to a maxima of 1 for ease of viewing. All spectra are shown for 10 min (blue), 1 h (green), and 4 h (red) after tryptophan-containing vesicles were equilibrated in buffer without tryptophan. Arrows indicate the changes of the spectra over time. (a) pH 2.4 (Trp+) and (b) pH 10.3 (Trp−).

DOI: 10.1021/acs.jpcb.8b09872
J. Phys. Chem. B 2019, 123, 170−179

To summarize, the four observations from Figure 4 all show that more Trp+ interacts with the lipid bilayer than Trp− and provide a strong indication that the Trp+ associated with the lipid bilayer is in a hydrophobic environment, close to the glycerol backbone region. The Trp− associated with the lipid bilayer is in a more hydrophilic environment at the time of elution from the columns, indicating Trp− associates with the lipid bilayer closer to the headgroup interfacial region.

The spectra in Figure 4 are clearly asymmetric and broadened, and so we further decomposed these spectra into the sum of two Gaussians, I_{lip} and I_{wat} (eq 1) to investigate the red-shifting of the fluorescence maxima over the time course of the experiment and determine what factors contributed to the overall observed red shifts seen in Figure 4. Because both the λ_{max} and intensity of each fluorescence peak changes based on local environment, we normalized I_{lip} and I_{wat} to concentrate solely on spectral energy shifts and peak broadening. We set the normalization factor for I_{lip} to 1.5 and I_{wat} to 1, so that the changes in the spectra over time would be clear, and plot this in Figure 5. As described above, I_{lip} (i.e., shorter λ_{max}) are representative of tryptophan near the glycerol backbone region of the lipid bilayer, and I_{wat} (i.e., longer λ_{max}) are representative of tryptophan in a hydrophilic environment (bulk water). All spectra are shown for 10 min (blue), 1 h (green), and 4 h (red) after elution from the size exclusion column. As seen in Figure 5a,b, I_{lip} experienced a 9 nm red shift for Trp+ over the time course of the experiment, compared to only a 2 nm red shift for Trp− over the same time. This indicates that Trp+ is in a more hydrophobic environment when the sample is eluted from the column, and the majority of the Trp+ leaves the hydrophobic lipid environment to enter the aqueous bulk solution. On the other hand, the smaller observed red shift for Trp− demonstrates that the negatively charged molecule is in a more hydrophilic environment at the time of column elution, and so changes to the chemical environment over the time course of the experiment are small. There was a slight broadening of the I_{wat} spectra for both Trp+ and Trp− that we attributed qualitatively to the greater diversity of environments that hydrated tryptophan experiences after it leaves the polar and zwitterionic headgroup region of the lipid and enters the aqueous bulk solution.

Because of our sequence of experimental steps, any tryptophan measured in Figures 4 and 5 must come from molecules that are associated, in some way, with the lipid bilayer vesicles as they are passed through the size exclusion column and into a buffer devoid of any tryptophan. The goal of this report is to determine the extent of tryptophan binding within some portion of the membrane interior, but tryptophan that had completely penetrated both leaflets of the bilayer structure and entered the interior of the vesicle would also travel through the size exclusion column with the vesicle and would be convoluted with fluorescence spectra that we have discussed so far, complicating our analysis. To eliminate this concern, we created tryptophan-containing vesicles by hydrating lipid films in the presence of the tryptophan stock solution, which created vesicles in which the concentration of tryptophan both inside and outside the vesicle was the same. We then performed the same series of experiments described above. We observed a significantly higher amount of tryptophan present in the solution, a lower degree of quenching, and more tryptophan in a hydrophilic environment after the vesicle was separated from the initial solution by size exclusion chromatography. These observations indicate that more tryptophan was present because it was trapped inside of the vesicles during the column elution. These molecules could not permeate through the hydrophobic core of the lipid membrane, and remained in the interior of the vesicles over the time course of the experiment. The same behavior was observed for Trp+ and Trp− with these experiments.

DISCUSSION

The purpose of this work is to determine the extent to which a charged tryptophan molecule permeates across the lipid bilayer at equilibrium versus partitions into the structure of the lipid bilayer at equilibrium. Further, if charged tryptophan does partition into the membrane, our goal is to determine approximately where it resides at equilibrium, which might account for the consistent observation that tryptophan side chains are found at the near-surface region of the membrane in transmembrane proteins. Finally, our goal is to determine any quantitative differences between positively and negatively charged molecules, which might account for the observation that CPPs predominantly carry a positive charge.

Previous calculations in which Trp+ and Trp− were simulated at various depths within the DOPC bilayer have demonstrated that there is a significant difference in free energy change, based on charge, when tryptophan enters the DOPC membrane. This is shown in Figure 6, where the x-axis represents the distance from the center of the bilayer, and where a DOPC molecule and solvating water molecules are drawn to scale to show their location along the membrane normal. While the PMF for Trp− is only slightly lower than that of solution (~2 kcal mol^{-1}), there is a significant drop in the PMF for Trp+ (~9 kcal mol^{-1}). There is also a significant difference in the location of the minimum PMF between the

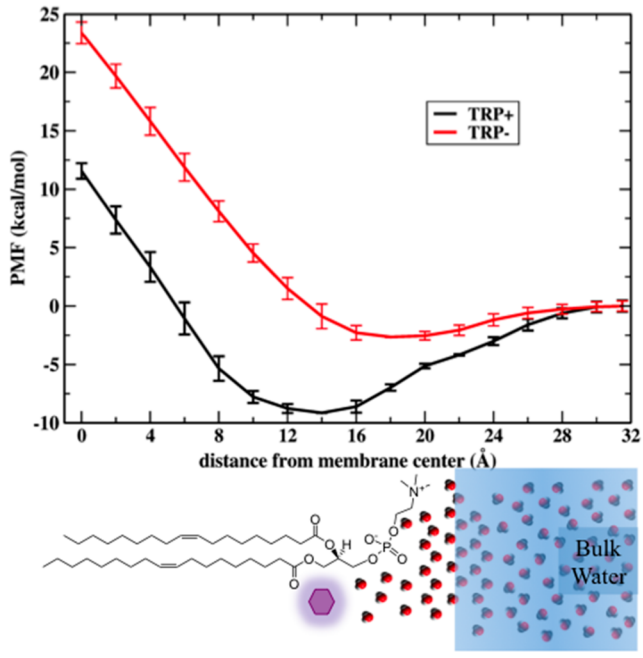

Figure 6. Computed free energy profile of Trp+ (black) and Trp− (red) as a function of distance from the membrane center. Below the x-axis is a DOPC molecule and magenta hexagon representing the approximate location of Trp+ locations of the lipid structure along the dimensions of the x-axis. Reprinted as adapted with permission from ref 21. Copyright 2015 American Chemical Society.

DOI: 10.1021/acs.jpcb.8b09872
J. Phys. Chem. B 2019, 123, 170−179

two molecules. Trp− achieves a minimum free energy very near the membrane−water interface, where it appears to be stabilized by the positively charged choline functional group. However, the minimum free energy position for Trp+ is significantly further into the membrane interior, much closer to the ester linkage that connects the high and low dielectric components of the lipid. At this position, Trp+ is stabilized not just by the negatively charged phosphate group on the lipid but also the electronegative oxygen atoms of the ester, that can also accept hydrogen bonds from the tryptophan backbone. This difference in equilibrium position of just 6 Å is a remarkable consequence of the molecular structure of the phospholipid forming the two-dimensional bilayer. No matter what charge the tryptophan carries, the PMF rises dramatically as soon as the molecule moves further into the interior of the lipid bilayer, increasing to ∼12−22 kcal mol^{-1} higher at the membrane center than in aqueous solution. This indicates that any tryptophan that does reside within the membrane is significantly more likely to exit the vesicle by moving back to the exterior of the vesicle, not through the membrane center and into the other leaflet.

These predictions from simulations are supported by our experiments. The initial fluorescence wavelength of charged tryptophan was significantly lower for Trp+ than Trp− (Figure 4), demonstrating that soon after vesicles had been removed from the spiked solution and were equilibrating in the tryptophan-free buffer, Trp+ was deeper into the low dielectric, hydrophobic interior of the membrane than Trp−. These results are confirmed by the greater degree of quenching of Trp+ fluorescence than that of Trp−, resulting from the position of Trp+ closer to the ester linkage (and therefore the quenching Br atoms) than Trp−. Because Trp− fluorescence was actually measured after the vesicles were passed through the size exclusion column, some Trp− was, in fact, closely associated with the vesicle. However, because the fluorescence energy of Trp− was near its value in pH 10.3 buffer, Trp− that moved through the size exclusion column with the vesicle appeared to be weakly associated with the surface region of the membrane near the positively charged choline. This Trp− then quickly dissociated from the vesicle surface, moving even further away from the vesicle, seen in the small decrease in fluorescence quenching in Figure 4b.

Furthermore, our experiments find that Trp+ reaches a higher equilibrium concentration than Trp− when partitioning in the lipid bilayer. This is predicted by the more attractive PMF calculated for Trp+ than Trp−, shown in Figure 6. Experimentally, this was estimated by determining the amount of tryptophan present in the sample at the time of elution. We determined the amount of Trp+ and Trp− present in the samples after the column elution by comparing the intensity of the 4 h time point spectra (in Figure 4) to the calibration curve for each buffer solution. We found 0.38 ± 0.04 mM Trp+ compared to only 0.076 ± 0.007 mM Trp− in solution after 4 h column elution. In other words, at equilibrium, 5 times as much Trp+ partitioned within the lipid bilayer membrane as Trp−. This result qualitatively agrees with the PMF calculations in Figure 6.

In our previous work, experimentally we explored Trp+, Trp−, and zwitterionic tryptophan (dissolved in solutions of pH 5.5 and 7.2). We also calculated the PMF of Trp+, Trp−, uncharged tryptophan, and a zwitterionic tryptophan molecule permeating through a DOPC lipid bilayer.[21] We found that the equilibrium concentration and calculated PMF of neutral tryptophan fell between those results for Trp+ and Trp−. Because our long-term interests are focused on the effect of molecular charge on membrane−molecule interactions, we did not investigate zwitterionic tryptophan in the current work. However, on the basis of our earlier work, we hypothesize that this molecule would partition itself in the lipid bilayer in an orientation that would allow the positively charged N-terminus to interact with the glycerol backbone region and the negatively charged C-terminus to interact with the choline group. In this scenario, we expect an equilibrium amount of zwitterionic tryptophan intermediate between Trp+ and Trp−.

The results presented here offer insight into the mechanism by which positively charged CPPs can penetrate a lipid bilayer membrane composed at least in part of zwitterionic phosphatidylcholine. In order to penetrate the lipid bilayer, there must be some initial interaction between the peptide and the bilayer. Although the lipid headgroup is zwitterionic, and can interact in essentially the same way with a molecule carrying either charge, the electronegative ester linkage directly under the headgroup will always favor a positively charged molecule. Moreover, the positively charged choline is more exposed to solvent compared to the phosphate. The phosphate, therefore, motivates the positively charged peptide to permeate more deeply into the membrane. If molecules of either charge can interact in some favorable way with the zwitterionic headgroup, shown in Figure 6, then dynamic fluctuations that expose the glycerol backbone to the headgroup region will favorably interact with positively charged molecules and, thus, select the positive charge for interactions deeper within the membrane. On the other hand, negatively charged molecules will be repelled from the negatively charged glycerol backbone region and remain closer to the water interface, where they can interact with the positively charged choline group on the lipid head. While Trp+ is not a large enough molecule to test further mechanisms of how CPPs, which are typically 15−30 amino acids in length, can further travel across the membrane, tryptophan is an ideal test for the role of charge near the lipid headgroup. Our results suggest that if the zwitterionic phosphocholine headgroup was reversed, i.e., the lipid headgroup has a quaternary amine adjacent to the bilayer interface and a phosphate that extends into the aqueous phase, interactions between Trp+ and the glycerol backbone would still allow Trp+ to partition and equilibrate within the membrane faster than Trp−. These experiments and simulations are underway in our laboratories.

CONCLUSIONS

In conclusion, we have demonstrated that the charge on a single tryptophan molecule, controlled by solution pH protonation of the terminal groups, controls the propensity of the molecule to partition into a DOPC lipid bilayer membrane. In the presence of Br-PC lipids, we found that more Trp+ fluorescence was quenched compared to Trp−, meaning Trp+ partitions closer to the glycerol backbone region, while Trp− partitions further away from the glycerol backbone region (closer to the water interface). When the tryptophan-containing phosphocoline lipid vesicles were re-equilibrated with a solution containing no tryptophan, both Trp+ and Trp− returned to the bulk solution and did not permeate through the lipid bilayer.

On the basis of these results, we conclude that independent of its charge, tryptophan partitions in the lipid bilayer and does not permeate through the hydrophobic core of the bilayer at

DOI: 10.1021/acs.jpcb.8b09872
J. Phys. Chem. B 2019, 123, 170−179

room temperature on the time scale of the experiment. We further conclude that the charge of tryptophan greatly affects the equilibrium reached when it partitions in the lipid bilayer; Trp+ has more favorable interactions with the interfacial region of the lipid bilayer than Trp− and therefore results in a greater amount of Trp+ partitioning in the lipid bilayer compared to Trp−. These results can offer insight into the mechanism by which CPPs are introduced and begin to penetrate lipid bilayers. These findings are consistent with the literature on tryptophan acting as an anchor for transmembrane proteins, and CPPs being composed of mostly positively charged amino acid residues.

AUTHOR INFORMATION

Corresponding Author

*E-mail: lwebb@cm.utexas.edu.

ORCID

Ron Elber: 0000-0001-7849-415X

Lauren J. Webb: 0000-0001-9999-5500

Notes

The authors declare no competing financial interest.

ACKNOWLEDGMENTS

This research was supported by the Welch Foundation (Grants F-1722 and F-1896) to L.J.W. and R.E. respectively, and the NIH (Grant GM111364) to L.J.W. and R.E. We acknowledge the Texas Materials Institute (TMI) at the University of Texas at Austin for the use of the Fluorolog 3 fluorimeter and Zetasizer Nano ZS DLS.

REFERENCES

(1) Deamer, D.; Kuzina, S. I.; Mikhailov, A. I.; Maslikova, E. I.; Seleznev, S. A. Origin of Amphiphilic Molecules and Their Role in Primary Structure Formation. *J. Evol. Biochem. Physiol.* **1991**, *27*, 212−217.

(2) Deamer, D. W. Role of Amphiphilic Compounds in the Evolution of Membrane Structure on the Early Earth. *Origins Life Evol. Biospheres* **1986**, *17*, 3−25.

(3) Morowitz, H. J.; Heinz, B.; Deamer, D. W. The Chemical Logic of a Minimum Protocell. *Origins Life Evol. Biospheres* **1988**, *18*, 281−287.

(4) Pohorille, A.; Deamer, D. Self-Assembly and Function of Primitive Cell Membranes. *Res. Microbiol.* **2009**, *160*, 449−456.

(5) Yang, N. J.; Hinner, M. J. Getting Across the Cell Membrane: An Overview for Small Molecules, Peptides, and Proteins. *Methods Mol. Biol.* **2015**, *1266*, 29−53.

(6) Lipinski, C. A.; Lombardo, F.; Dominy, B. W.; Feeney, P. J. Experimental and Computational Approaches to Estimate Solubility and Permeability in Drug Discovery and Development Settings. *Adv. Drug Delivery Rev.* **1997**, *23*, 3−25.

(7) Veber, D. F.; Johnson, S. R.; Cheng, H.-Y.; Smith, B. R.; Ward, K. W.; Kopple, K. D. Molecular Properties That Influence the Oral Bioavailability of Drug Candidates. *J. Med. Chem.* **2002**, *45*, 2615−2623.

(8) Guimarães, C. R. W.; Mathiowetz, A. M.; Shalaeva, M.; Goetz, G.; Liras, S. Use of 3D Properties to Characterize Beyond Rule-of-5 Property Space for Passive Permeation. *J. Chem. Inf. Model.* **2012**, *52*, 882−890.

(9) Al-Awqati, Q. One Hundred Years of Membrane Permeability: Does Overton Still Rule? *Nat. Cell Biol.* **1999**, *1*, E201−E202.

(10) Li, L.; Vorobyov, I.; Allen, T. W. The Different Interactions of Lysine and Arginine Side Chains with Lipid Membranes. *J. Phys. Chem. B* **2013**, *117*, 11906−11920.

(11) Bemporad, D.; Luttmann, C.; Essex, J. W. Computer Simulation of Small Molecule Permeation across a Lipid Bilayer: Dependence on Bilayer Properties and Solute Volume, Size, and Cross-Sectional Area. *Biophys. J.* **2004**, *87*, 1−13.

(12) Chakrabarti, A. C.; Deamer, D. W. Permeability of Lipid Bilayers to Amino Acids and Phosphate. *Biochim. Biophys. Acta, Biomembr.* **1992**, *1111*, 171−177.

(13) Wimley, W. C.; White, S. H. Experimentally Determined Hydrophobicity Scale for Proteins at Membrane Interfaces. *Nat. Struct. Mol. Biol.* **1996**, *3*, 842.

(14) MacCallum, J. L.; Bennett, W. F. D.; Tieleman, D. P. Partitioning of Amino Acid Side Chains into Lipid Bilayers: Results from Computer Simulations and Comparison to Experiment. *J. Gen. Physiol.* **2007**, *129*, 371.

(15) Chakrabarti, A. C. Permeability of Membranes to Amino Acids and Modified Amino Acids: Mechanisms Involved in Translocation. *Amino Acids* **1994**, *6*, 213−229.

(16) Yesylevskyy, S.; Marrink, S.-J.; Mark, A. E. Alternative Mechanisms for the Interaction of the Cell-Penetrating Peptides Penetratin and the TAT Peptide with Lipid Bilayers. *Biophys. J.* **2009**, *97*, 40−49.

(17) Vivès, E.; Schmidt, J.; Pèlegrin, A. Cell-Penetrating and Cell-Targeting Peptides in Drug Delivery. *Biochim. Biophys. Acta, Rev. Cancer* **2008**, *1786*, 126−138.

(18) Huang, K.; García, A. E. Free Energy of Translocating an Arginine-Rich Cell-Penetrating Peptide across a Lipid Bilayer Suggests Pore Formation. *Biophys. J.* **2013**, *104*, 412−420.

(19) Herce, H. D.; Garcia, A. E.; Litt, J.; Kane, R. S.; Martin, P.; Enrique, N.; Rebolledo, A.; Milesi, V. Arginine-Rich Peptides Destabilize the Plasma Membrane, Consistent with a Pore Formation Translocation Mechanism of Cell-Penetrating Peptides. *Biophys. J.* **2009**, *97*, 1917−1925.

(20) Herce, H. D.; Garcia, A. E. Cell Penetrating Peptides: How Do They Do It? *J. Biol. Phys.* **2007**, *33*, 345−356.

(21) Cardenas, A. E.; Shrestha, R.; Webb, L. J.; Elber, R. Membrane Permeation of a Peptide: It is Better to be Positive. *J. Phys. Chem. B* **2015**, *119*, 6412−20.

(22) White, S. H.; Wimley, W. C. Membrane Protein Folding and Stability: Physical Principles. *Annu. Rev. Biophys. Biomol. Struct.* **1999**, *28*, 319−365.

(23) Killian, J. A.; von Heijne, G. How Proteins Adapt to a Membrane−Water Interface. *Trends Biochem. Sci.* **2000**, *25*, 429−434.

(24) Yau, W.-M.; Wimley, W. C.; Gawrisch, K.; White, S. H. The Preference of Tryptophan for Membrane Interfaces. *Biochemistry* **1998**, *37*, 14713−14718.

(25) Sanchez, K. M.; Kang, G.; Wu, B.; Kim, J. E. Tryptophan-Lipid Interactions in Membrane Protein Folding Probed by Ultraviolet Resonance Raman and Fluorescence Spectroscopy. *Biophys. J.* **2011**, *100*, 2121−2130.

(26) Granseth, E.; von Heijne, G.; Elofsson, A. A study of the Membrane-Water Interface Region of Membrane Proteins. *J. Mol. Biol.* **2005**, *346*, 377−85.

(27) Landolt-Marticorena, C.; Williams, K. A.; Deber, C. M.; Reithmeier, R. A. F. Non-random Distribution of Amino Acids in the Transmembrane Segments of Human Type I Single Span Membrane Proteins. *J. Mol. Biol.* **1993**, *229*, 602−608.

(28) Chamberlain, A. K.; Lee, Y.; Kim, S.; Bowie, J. U. Snorkeling Preferences Foster an Amino Acid Composition Bias in Transmembrane Helices. *J. Mol. Biol.* **2004**, *339*, 471−479.

(29) Arkin, I. T.; Brunger, A. T. Statistical Analysis of Predicted Transmembrane α-Helices. *Biochim. Biophys. Acta, Protein Struct. Mol. Enzymol.* **1998**, *1429*, 113−128.

(30) Jobin, M.-L.; Blanchet, M.; Henry, S.; Chaignepain, S.; Manigand, C.; Castano, S.; Lecomte, S.; Burlina, F.; Sagan, S.; Alves, I. D. The Role of Tryptophans on the Cellular Uptake and Membrane Interaction of Arginine-Rich Cell Penetrating Peptides. *Biochim. Biophys. Acta, Biomembr.* **2015**, *1848*, 593−602.

(31) de Jesus, A. J.; Allen, T. W. The Role of Tryptophan Side Chains in Membrane Protein Anchoring and Hydrophobic Mismatch. *Biochim. Biophys. Acta, Biomembr.* **2013**, *1828*, 864−876.

DOI: 10.1021/acs.jpcb.8b09872
J. Phys. Chem. B 2019, 123, 170−179

(32) Ulmschneider, J. P.; Andersson, M.; Ulmschneider, M. B. Determining Peptide Partitioning Properties via Computer Simulation. *J. Membr. Biol.* **2011**, *239*, 15−26.
(33) Ulmschneider, M. B.; Sansom, M. S. P. Amino Acid Distributions in Integral Membrane Protein Structures. *Biochim. Biophys. Acta, Biomembr.* **2001**, *1512*, 1−14.
(34) Arseniev, A. S.; Barsukov, I. L.; Bystrov, V. F.; Lomize, A. L.; Ovchinnikov, Y. A. 1H-NMR Study of Gramicidin A Transmembrane Ion Channel. Head-to-Head Right-Handed, Single-Stranded Helices. *FEBS Lett.* **1985**, *186*, 168−184.
(35) Cowan, S. W.; Schirmer, T.; Rummel, G.; Steiert, M.; Ghosh, R.; Pauptit, R. A.; Jansonius, J. N.; Rosenbusch, J. P. Crystal Structures Explain Functional Properties of Two E. Coli Porins. *Nature* **1992**, *358*, 727.
(36) Deisenhofer, J.; Michel, H. The Photosynthetic Reaction Centre From the Purple Bacterium Rhodopseudomonas viridis. *EMBO J.* **1989**, *8*, 2149−2170.
(37) *Probing Membrane Protein Structure and Dynamics by Fluorescence Spectroscopy. Encyclopedia of Analytical Chemistry [Online]*; Wiley & Sons, https://onlinelibrary.wiley.com/doi/abs/10.1002/9780470027318.a9353 (accessed Aug 1, 2018).
(38) Lakowicz, J. R. *Principles of Fluorescence Spectroscopy*; Springer: New York, 2006; pp 205−235.
(39) Vivian, J. T.; Callis, P. R. Mechanisms of Tryptophan Fluorescence Shifts in Proteins. *Biophys. J.* **2001**, *80*, 2093−2109.
(40) Valeur, B.; Weber, G. Resolution of the Fluorescence Excitation Spectrum of Indole into the 1La and 1Lb Excitation Bands. *Photochem. Photobiol.* **1977**, *25*, 441−444.
(41) Soni, S. P.; Adu-Gyamfi, E.; Yong, S. S.; Jee, C. S.; Stahelin, R. V. The Ebola Virus Matrix Protein Deeply Penetrates the Plasma Membrane: An Important Step in Viral Egress. *Biophys. J.* **2013**, *104*, 1940−1949.
(42) Pfefferkorn, C. M.; Walker, R. L.; He, Y.; Gruschus, J. M.; Lee, J. C. Tryptophan Probes Reveal Residue-Specific Phospholipid Interactions of Apolipoprotein C-III. *Biochim. Biophys. Acta, Biomembr.* **2015**, *1848*, 2821−2828.
(43) Gable, J. E.; Schlamadinger, D. E.; Cogen, A. L.; Gallo, R. L.; Kim, J. E. Fluorescence and UV Resonance Raman Study of Peptide-Vesicle Interactions of Human Cathelicidin LL-37 and its F6W and F17W Mutants. *Biochemistry* **2009**, *48*, 11264−11272.
(44) Lakowicz, J. R. *Principles of Fluorescence Spectroscopy*; Springer: New York, 2006; pp 331−351.
(45) Liu, L.-P.; Deber, C. M. Anionic Phospholipids Modulate Peptide Insertion into Membranes. *Biochemistry* **1997**, *36*, 5476−5482.
(46) Mishra, V. K.; Palgunachari, M. N. Interaction of Model Class A1, Class A2, and Class Y Amphipathic Helical Peptides with Membranes. *Biochemistry* **1996**, *35*, 11210−11220.
(47) Macdo, Z. S.; Furquim, T. A.; Ito, A. S. Estimation of Average Depth of Penetration of Melanotropins in Dimyristoylphosphatidylglycerol Vesicles. *Biophys. Chem.* **1996**, *59*, 193−202.
(48) Lewis, R. N. A. H.; McElhaney, R. N. Fourier Transform Infrared Spectroscopy in the Study of Lipid Phase Transitions in Model and Biological Membranes: Practical Considerations. In *Methods in Membrane Lipids*; Dopico, A. M., Ed.; Humana Press: NJ, 2007; pp 207−227.
(49) Bystrov, V. F.; Shapiro, Y. E.; Viktorov, A. V.; Barsukov, L. I.; Bergelson, L. D. 31P-NMR Signals From Inner and Outer Surfaces of Phospholipid Membranes. *FEBS Lett.* **1972**, *25*, 337−338.

DOI: 10.1021/acs.jpcb.8b09872
J. Phys. Chem. B 2019, 123, 170−179